



# High-pressure study of the conversion of NH<sub>3</sub>/H<sub>2</sub> mixtures in a flow reactor

Pedro García-Ruiz, Daniel Castejón, Miguel Abengochea, Rafael Bilbao, María U. Alzueta\*

Aragón Institute of Engineering Research (I3A), Department of Chemical and Environmental Engineering, University of Zaragoza, 50018 Zaragoza, Spain

## ARTICLE INFO

**Keywords:**  
Ammonia  
Hydrogen  
N<sub>2</sub>O  
High Pressure  
Kinetic Modeling

## ABSTRACT

Carbon free fuels such as hydrogen (H<sub>2</sub>) and ammonia (NH<sub>3</sub>) will probably play a fundamental role owing to their potential for clean combustion without CO<sub>2</sub> emissions. To contribute to the knowledge and development of technologies based on carbon free combustion, the present work deals with an experimental and kinetic analysis of ammonia oxidation in its mixtures with hydrogen at high pressure (up to 40 bar), in the 250–1250 K temperature range using a quartz tubular reactor and argon as bath gas. The impact of temperature, pressure, stoichiometry and H<sub>2</sub>/NH<sub>3</sub> ratio on the concentrations of NH<sub>3</sub>, NO, NO<sub>2</sub>, N<sub>2</sub>O, and N<sub>2</sub> obtained as main products of oxidation has been analyzed. The main results indicate that either increasing pressure, H<sub>2</sub>/NH<sub>3</sub> ratio or oxygen availability results in a shift of NH<sub>3</sub> and H<sub>2</sub> conversion to lower temperatures. The NH<sub>3</sub> and H<sub>2</sub> consumptions are promoted by the reactions that produce NH<sub>2</sub>, H, OH, O, HO<sub>2</sub> and HNO species and inhibited by reactions that form H<sub>2</sub>O, NH<sub>3</sub>, NO, H<sub>2</sub>NO and O<sub>2</sub> species. The pressure effect is particularly significant in the low range of pressures studied. The main ammonia oxidation nitrogen products are N<sub>2</sub> and N<sub>2</sub>O, while NO and NO<sub>2</sub> concentrations are below the detection limit under all considered conditions. N<sub>2</sub>O formation is favored by increasing stoichiometry, pressure and H<sub>2</sub>/NH<sub>3</sub> ratio. The experimental results are simulated and interpreted in terms of a literature detailed chemical kinetic mechanism, which, in general, is able to describe quite well both the H<sub>2</sub> and NH<sub>3</sub> conversion profiles under the studied conditions.

## 1. Introduction

Net-zero emission fuel use is expected to grow by 2050. Hydrogen is projected to account for 28% of the transport energy required for that date [1]. In this context, fuels such as H<sub>2</sub> and NH<sub>3</sub> play a critical role due to their potential for clean combustion without CO<sub>2</sub> emissions, and H<sub>2</sub>O and N<sub>2</sub> as reaction products, through 4NH<sub>3</sub> + 3O<sub>2</sub> ⇌ 2N<sub>2</sub> + 6H<sub>2</sub>O (R1) [2] and 2H<sub>2</sub> + O<sub>2</sub> ⇌ 2H<sub>2</sub>O (R2). The advantages of using NH<sub>3</sub> in power generation turbine systems [3] or combustion engines include established manufacture, safe transport, storage and developed infrastructures [4–6]. The use of NH<sub>3</sub> as a fuel also presents some drawbacks such as low heating value and flame speed [7], and high autoignition temperature [8] than other hydrocarbon fuels, together with the possible NO<sub>x</sub> and unburned NH<sub>3</sub> emissions [4,9]. In this sense, a possible solution to palliate these barriers and improve NH<sub>3</sub> combustion characteristics is to mix it with other fuels: e.g. H<sub>2</sub> [6,10–17], CH<sub>4</sub> [3,7,18–20] and DME [21–23]. Despite the fact that the CH<sub>4</sub> and DME addition improves the combustion properties of ammonia mixtures, some CO<sub>2</sub> is still emitted. In this line, NH<sub>3</sub>/H<sub>2</sub> mixtures have a special interest because H<sub>2</sub> is the most effective additive to enhance the NH<sub>3</sub>

burning velocity [24] and the cleanest of previously mentioned fuels in terms of carbon emissions. At the same time, mixing NH<sub>3</sub> and H<sub>2</sub> improves the safety of H<sub>2</sub> combustion [13,14]. In general, the addition of H<sub>2</sub> to the fuel mixture, even in small fractions, enhances the ignition of NH<sub>3</sub>, as has been reported even for small amounts of H<sub>2</sub> to the fuel mixture, such as 5 % [1,16]. This enhancement is attributed to the increase in H, O and OH radicals produced by adding H<sub>2</sub> to the mixture. This is consistent with the fact that the reaction NH<sub>3</sub> + OH ⇌ NH<sub>2</sub> + H<sub>2</sub>O (R3) appears as an important NH<sub>3</sub> consumption reaction particularly when H<sub>2</sub> is added [12]. Alturaifi et al. [12] identified some important equations that cause this increase in H-radicals such as NH<sub>2</sub> + H<sub>2</sub> ⇌ NH<sub>3</sub> + H (-R4). Additionally, the use of NH<sub>3</sub>/H<sub>2</sub> blends avoids the production of HCN and has a lower NO production potential [25] than the mixture with hydrocarbons. However, compared with pure NH<sub>3</sub> and pure H<sub>2</sub> combustion, the NH<sub>3</sub>/H<sub>2</sub> combustion increases NO<sub>x</sub> and unburn NH<sub>3</sub> emissions during combustion [1], and this is one of the most noticeable challenges for NH<sub>3</sub>/H<sub>2</sub> implementation as an energy source. At this point, it is important to note that working at high pressures can result in lower NO emissions [25]. In the meantime, further work is needed to develop and test a reaction kinetic mechanism to understand better the

\* Corresponding author.

E-mail address: [p.garcia@unizar.es](mailto:p.garcia@unizar.es) (M.U. Alzueta).

<https://doi.org/10.1016/j.proci.2024.105726>

Received 30 November 2023; Accepted 29 July 2024

Available online 19 August 2024

1540-7489/© 2024 The Author(s). Published by Elsevier Inc. on behalf of The Combustion Institute. This is an open access article under the CC BY-NC-ND license (<http://creativecommons.org/licenses/by-nc-nd/4.0/>).

chemistry of  $\text{NH}_3$  in its combustion with  $\text{H}_2$ , since there are discrepancies in the most accurate models provided in the literature [12], and this is one of the aims of this work. In the recent literature, a number of experimental and kinetic works on  $\text{NH}_3/\text{H}_2$  mixtures combustion at low pressure (from 0.05 to 5 bar), performed using different experimental set-ups, can be found, although only two of them in flow reactors to our knowledge. It should be noted that most of the works in the literature are focused on flame studies including stability, flame structure, laminar burning velocity, ignition delay times and  $\text{NO}_x$  formation. Nevertheless, there is a gap in knowledge regarding studies performed using plug-flow reactors. From an industrial application point of view, it is important to mention the works carried out at pressures over 5 bar are still scarce. Studies at high pressure available include works in a rapid compression machine (RCM) [16,26,27], a swirl burner [28], a combustion tube [29] and a cylindrical combustor [30]. It can also be mentioned the numerical study of Li et al. [31] that focused on  $\text{NO}_x$  emissions characteristics at high-pressure. Dai et al. [16] determined ignition delay times of the  $\text{NH}_3/\text{H}_2$  oxidation for different  $\text{H}_2$  fractions (5% and 10%) at 20 and 60 bar from reducing to oxidizing conditions ( $\lambda = 0.33, 0.5, 1$  and  $2$ ) in a RCM and elevated temperature from 1040 K to 1210 K. He et al. [26] studied the autoignition properties and species concentration of  $\text{NH}_3/\text{H}_2$  oxidation in argon at 20 and 60 bar from  $\lambda = 0.67$  to  $\lambda = 2$  in a RCM and elevated temperature from 950 K to 1150 K. Pochet et al. [27] studied the influence of  $\text{H}_2$  addition to  $\text{NH}_3$  on ignition delay times at 43.4 and 65.5 bar at  $\lambda = 2$  and  $\lambda = 5$  in a RCM and temperatures from 1000 K to 1100 K. Valera-Medina et al. [28], Li et al. [29] and Mei et al. [30] performed the other high-pressure experimental and numerical works mentioned above, up to 10 bar, in which  $\text{NO}_x$  formation, species concentration, flame morphology, laminar burning velocities were determined. Increasing the pressure can reduce the unburned  $\text{NH}_3$  and  $\text{NO}$  production [17,25]. However, the effect on  $\text{N}_2\text{O}$  formation is not so clear and results by Wang et al. [25] in a pressure study, up to 5 bar, have shown different trends compared to results obtained in the oxidation of  $\text{NH}_3/\text{CH}_4$  mixtures [32]. So,  $\text{N}_2\text{O}$  production at high pressures deserves further study, as considered in the present work.

In this scenario, the objective of this work is to provide new experimental data on the combustion of  $\text{NH}_3/\text{H}_2$  mixtures in a high pressure and temperature quartz flow reactor setup, analyzing the effect as main variables of temperature, pressure, oxygen excess and  $\text{H}_2/\text{NH}_3$  ratios. Experimental results are interpreted in terms of a chemical kinetic mechanism taken from previous work [32], to understand the chemistry and product formation, and to determine the main reaction pathways through which reactions proceed.

## 2. Methodology

Conversion of reactants and formed products during the combustion of a  $\text{NH}_3/\text{H}_2$  mixture are studied at high pressure (10, 20, 30 and 40 bar) in a well-controlled laboratory-scale quartz flow reactor setup. Additionally, to pressure, other variables considered include stoichiometry (stoichiometric,  $\lambda = 1$ , and oxidizing,  $\lambda = 3$ , conditions), and the  $\text{H}_2/\text{NH}_3$  ratio (0.5, 1 and 2) which means using  $\text{H}_2$  nominal concentrations of 500 ppm, 1000 ppm and 2000 ppm for an  $\text{NH}_3$  nominal concentration of 1000 ppm in a wide range of temperatures (from 250 K to 1250 K). The experimental set-up has been used in success and described in previous works e.g. [32–35]. The oxygen excess ratio ( $\lambda$ ) is defined on the basis of the  $\text{NH}_3$  oxidation reaction to  $\text{N}_2$  (R1):

$$\lambda = [\text{O}_2]_{\text{inlet}}/[\text{O}_2]_{\text{stoichiometric}} \quad (1)$$

and the flow rate is 1 L(STP)/min, and implies a temperature and pressure dependent gas residence time in the isothermal reaction zone:

$$\tau_r \text{ (s)} = 231.6 \cdot P(\text{bar})/T(\text{K}), \quad (2)$$

where  $P$  and  $T$  are the gas pressure and temperature. Experiments are performed using argon as a bath gas, which allows us to determine the

molecular nitrogen formed during reaction, and to calculate the nitrogen atoms balance. In the experiments,  $\text{H}_2$ ,  $\text{O}_2$ , and  $\text{N}_2$  concentrations are analyzed and quantified with a gas micro-chromatograph (Agilent Technologies) and a  $\text{NH}_3/\text{NO}/\text{NO}_2/\text{N}_2\text{O}$  continuous analyzer (ABB, model: Advance Optima AO2020). The estimated measurement uncertainty is  $\pm 5\%$ , but not less than 5 ppm for the continuous analyzer and 10 ppm for the gas micro-chromatograph. Table 1 summarizes the experimental initial conditions. Sets 5 and 5R correspond to similar experiments to evaluate repetitiveness.

The experimental results have been analyzed using a gas-phase chemical kinetic mechanism, to describe the oxidation of  $\text{NH}_3/\text{CH}_4$  under high-pressure conditions, without modification [32]. Fig. S1 of the supplementary material shows an example of the validation of the present mechanism against literature data [36] for a plug flow reactor under atmospheric conditions. Calculations have been carried out using the plug-flow reactor (PFR) model of the Chemkin Pro suite [37], using the initial conditions for each experiment, as listed in Table 1, and a “fix gas temperature” type problem, using the nominal reaction temperature at the flat temperature zone, since similar results were obtained with and without the measured temperature profiles.

## 3. Results

### 3.1. Effect of pressure

Fig. 1 and 2 show the conversion of  $\text{NH}_3$  and  $\text{H}_2$  respectively as a function of temperature for different pressures (from 10 to 40 bar),  $\text{H}_2/\text{NH}_3$  ratios (0.5, 1 and 2), and oxygen excess ratios ( $\lambda = 1$  and 3). Keeping the rest of the conditions similar, each increase of pressure of 10 bar (from 10 to 40 bar) makes the  $\text{NH}_3$  conversion onset for  $\lambda = 1$  to vary to lower temperatures, following the sequence 50 K, 50 K and 15 K (temperatures of respectively 925 K, 875 K, 825 K and 810 K) for  $\text{H}_2/\text{NH}_3 = 1$ ; Similarly, under oxidizing conditions ( $\lambda = 3$ ) the shift in temperature values is 50 K, 25 K and 25 K (925 K  $\rightarrow$  875 K  $\rightarrow$  850 K  $\rightarrow$  825 K) for  $\text{H}_2/\text{NH}_3 = 0.5$ . For  $\text{H}_2/\text{NH}_3 = 1$ , the reduction is 50 K, 25 K and 0 K (875 K  $\rightarrow$  825 K  $\rightarrow$  800 K  $\rightarrow$  800 K) and for the higher  $\text{H}_2/\text{NH}_3$  ratio studied is 25 K, 25 K, 0 K (850 K  $\rightarrow$  825 K  $\rightarrow$  800 K  $\rightarrow$  800 K). Similar observations can be done for the onset temperature of the  $\text{H}_2$  oxidation reaction and for each pressure increase under the same conditions. As can be seen, the reaction onset temperature of  $\text{NH}_3$  oxidation when mixed with  $\text{H}_2$  shows a pressure dependence, as pointed out by other authors [16,26]. He et al. [26] reported that increasing the pressure results in an increase in reactivity and a decrease in the ignition delay time by a factor of 10 using a RCM system in the 20–40 bar range and 5% of  $\text{H}_2$  in the mixture. Generally, the onset temperature decreases with increasing pressure at all conditions studied, as also observed with

**Table 1**

Matrix of mixture compositions in the present work. (Concentrations in ppm).

Set	$\text{NH}_3$	$\text{H}_2$	$\text{O}_2$	P (bar)	$\lambda$
1	1092	421	2933	10	2.85
2	1064	422	2906	20	2.89
3	1067	424	3036	30	3.00
4	848	432	2866	40	3.35
5	1084	914	1234	10	0.97
5R	1092	873	1239	10	0.99
6	1081	814	1197	20	0.98
7	1038	972	1184	30	0.94
8	1102	879	1212	40	0.96
9	1107	899	3857	10	3.01
10	1096	867	3746	20	2.98
11	1027	936	3658	30	2.95
12	1059	891	3602	40	2.91
13	885	1851	5135	10	3.23
14	874	1854	5197	20	3.28
15	882	1899	5133	30	3.19
16	858	1806	5113	40	3.31

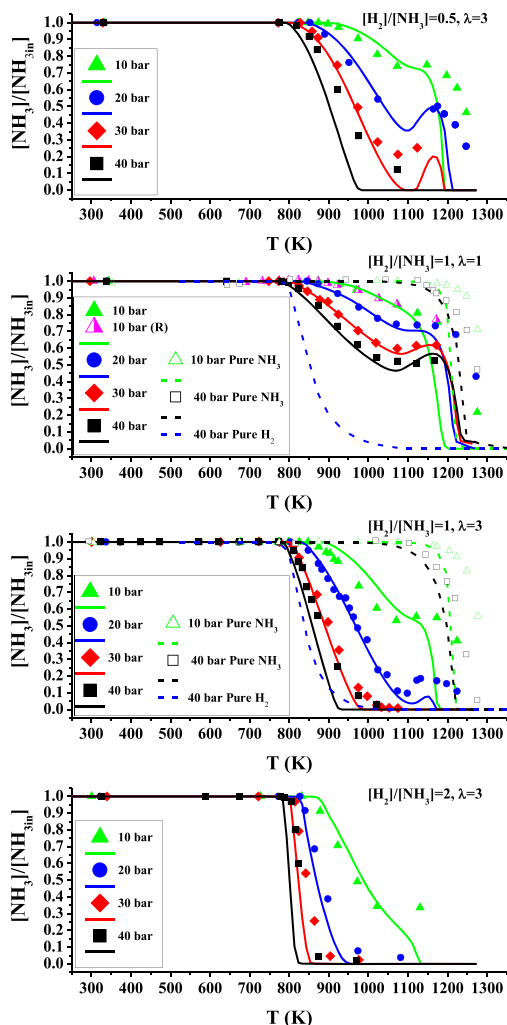


Fig. 1.  $\text{NH}_3$  conversion as a function of temperature for different pressures (10–40 bar), sets 1–16 in Table 1.

pure  $\text{NH}_3$  oxidation at high pressure [34]. In Fig. 1 and 2 it should be noted that the effect of pressure on the  $\text{NH}_3$  and  $\text{H}_2$  reaction onset temperature is slightly minor as the  $\text{H}_2/\text{NH}_3$  ratio increases, under the studied conditions. The same trend in reaction onset temperature for  $\text{NH}_3$  and  $\text{H}_2$  oxidation can be seen with increasing excess oxygen from stoichiometric ( $\lambda = 1$ ) to oxidizing conditions ( $\lambda = 3$ ), for  $\text{H}_2/\text{NH}_3 = 1$ . Nevertheless, for  $\text{NH}_3$  oxidation, the pressure has a significant effect on the unburned  $\text{NH}_3$ . It can be observed that the conversion of  $\text{NH}_3$  is much higher at higher pressures at intermediate and high temperatures. This is not the case for  $\text{H}_2$  oxidation, which achieves complete conversion under all studied conditions. The pressure effect is also found in the case of oxidation of pure  $\text{NH}_3$  [34], although less important than for the  $\text{H}_2/\text{NH}_3$  mixture. For pure  $\text{NH}_3$ , at 10 bar, unburned  $\text{NH}_3$  is found at high temperatures (1250–1300 K), while at 40 bar, there is no unburned  $\text{NH}_3$  under oxidizing conditions at 1275 K. The effect of  $\text{H}_2$  addition on the  $\text{NH}_3$  ignition is noticeable, as the  $\text{NH}_3$  reaction onset temperature decreases 250 K–350 K for the studied conditions when compared to pure  $\text{NH}_3$  [17,34], in agreement with other authors findings [1,12,16]. Apart from pressure, the oxygen availability logically has a remarkable effect in the unburned  $\text{NH}_3$ , which is much larger at  $\text{H}_2/\text{NH}_3 = 1$  and  $\lambda = 1$  than in the rest of the conditions for  $\lambda = 3$ , even in the case of  $\text{H}_2/\text{NH}_3 = 0.5$ , in the line with the results of Osipova et al. [17] in a jet stirred reactor at atmospheric pressure.

In general, the model reproduces quite well the reaction onset temperature and the main trends of  $\text{NH}_3$  and  $\text{H}_2$  consumption, for the

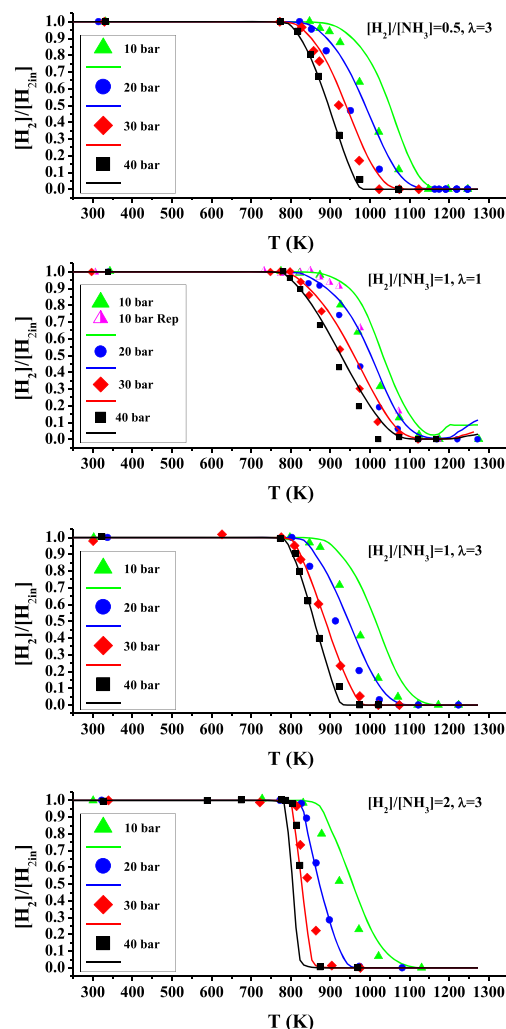


Fig. 2.  $\text{H}_2$  conversion as a function of temperature for different pressures (10–40 bar), sets 1–16 in Table 1.

different pressures at  $\lambda = 1$  and 3 conditions of Fig. 1 and 2. The model shows that the main  $\text{NH}_3$  consumption pathways are  $\text{NH}_3 \rightarrow \text{NH}_2 \rightarrow \text{N}_2$  and  $\text{NH}_3 \rightarrow \text{NH}_2 \rightarrow \text{H}_2\text{NO} \rightarrow \text{HNO}/\text{HONO} \rightarrow \text{NO} \rightarrow \text{NO}_2 \rightarrow \text{N}_2\text{O}$ . The consumption pathway of  $\text{H}_2$  is  $\text{H}_2 \rightarrow \text{H} \rightarrow \text{HO}_2 \rightarrow \text{OH} \rightarrow \text{H}_2\text{O}$  (Fig. S2–S5). The autoignition enhancement of ammonia occurs due to the increase in H, O and OH radicals by the addition of  $\text{H}_2$  [1,12]. This increase in the H/O radical pool leads to a higher consumption of  $\text{NH}_3$  and  $\text{NH}_2$ . The model is also able to reproduce the decrease of  $\text{NH}_3$  consumption produced at 900 K–1100 K as can be observed in Fig. 1 in the three first cases ( $\text{H}_2/\text{NH}_3 = 0.5$  and 1). The main  $\text{NH}_3$  consumption reaction is  $\text{NH}_3 + \text{OH} \rightleftharpoons \text{NH}_2 + \text{H}_2\text{O}$  (R3) and the two main  $\text{NH}_3$  production reactions are  $\text{NH}_2 + \text{H}_2 \rightleftharpoons \text{NH}_3 + \text{H}$  (-R4) and  $\text{H}_2\text{NO} + \text{NH}_2 \rightleftharpoons \text{HNO} + \text{NH}_3$  (R5), when 10 % of  $\text{NH}_3$  is consumed (Fig. S2–S5).  $\text{H}_2$  is consumed by  $\text{NH}_2 + \text{H}_2 \rightleftharpoons \text{NH}_3 + \text{H}$  (-R4) and  $\text{OH} + \text{H}_2 \rightleftharpoons \text{H} + \text{H}_2\text{O}$  (R6), under the same conditions (Fig. S2–S5).  $\text{NH}_3$  and  $\text{H}_2$  consumption is promoted by reactions (-R4) and (R6) while (R3) and (R5) imply inhibition effects (Fig. S6–S9). When  $\text{H}_2$  is added, the concentration of the O/H radical pool is increased by chain branching reactions. The  $\text{H}_2$  consumption reactions provoke the increase in H radical via (-R4) and (R6), which is consumed mainly by its reaction with  $\text{NO}_2$  and  $\text{O}_2$  producing OH:  $\text{NO}_2 + \text{H} \rightleftharpoons \text{NO} + \text{OH}$  (R7), and  $\text{HO}_2 + \text{H} + \text{O}_2 (+\text{M}) \rightleftharpoons \text{HO}_2 (+\text{M})$  (R8) respectively. The  $\text{HO}_2$ , produced by (R8) and  $\text{HNO} + \text{O}_2 \rightleftharpoons \text{HO}_2 + \text{NO}$  (R9), leads to the formation of OH by reaction with NO:  $\text{HO}_2 + \text{NO} \rightleftharpoons \text{NO}_2 + \text{OH}$  (R10). In addition to this reaction,  $\text{HONO} (+\text{M}) \rightleftharpoons \text{NO} + \text{OH} (+\text{M})$  (-R11) also contributes to OH formation (Fig. S2–S5). To a minor extent, O radicals are formed by the

reaction  $\text{H} + \text{O}_2 \rightleftharpoons \text{O} + \text{OH}$  (R12), which efficiently promotes  $\text{NH}_3$  and  $\text{H}_2$  conversion, and are consumed forming OH and H radicals. OH radicals are then consumed by (R3) and (R6) (Fig. S2-S5). Reaction (R7) has an inhibitory effect on  $\text{NH}_3$  and  $\text{H}_2$  consumption under all studied conditions, while (R8) only under the lowest pressure studied, showing a pressure dependence (Fig. S6-S9). However, in the 900–1200 K range, the  $\text{H}_2$  is depleted and the rate of OH radical production decreases due to the decrease in H radicals following the same trend as  $\text{NH}_3$  consumption. In the decrease of the O/H radical pool, the species NO,  $\text{NO}_2$ , HNO,  $\text{H}_2\text{NO}$ , HONO, H,  $\text{HO}_2$ , and O are involved. In more detail, in temperatures lower than the one of the “NTC” behavior, the produced H radicals are consumed mainly by the reaction  $\text{NO}_2 + \text{H} \rightleftharpoons \text{NO} + \text{OH}$  that produces OH radicals and to more extent by reaction  $\text{H} + \text{O}_2 (+\text{M}) \rightleftharpoons \text{HO}_2 (+\text{M})$  that contributed to OH formation through  $\text{HO}_2 + \text{NO} \rightleftharpoons \text{NO}_2 + \text{OH}$  reaction, as mentioned before. These reactions represent the main source of OH radicals. However, in the “NTC” area, the reaction rate of these H consumption reactions decreased by one order of magnitude, and this decrease in the reactions forming OH radical provokes the reduction in the  $\text{NH}_3$  consumption.

When  $\text{H}_2$  is fully consumed before the  $\text{NH}_3$  is depleted, the rate of  $\text{NH}_3$  consumption decreases due to the decrease in OH radicals, and thus a saddle point is produced and, in some cases, even a small increase in the  $\text{NH}_3$  concentration in the reactor outlet at the highest temperatures studied (950 K–1250 K), similar to the NTC behavior of oxygenated fuels. The reason why this is not seen at the higher pressures studied is owing to the fact that  $\text{NH}_3$  and  $\text{H}_2$  are completely burned at the same temperature. Osipova et al. [17] reported that the O/H radical pool starts to form at lower temperatures in the presence of  $\text{H}_2$  under atmospheric pressure conditions. It appears that at high pressure this effect also occurs, and is responsible for the decrease in the onset temperature of the  $\text{NH}_3$  conversion compared to the pure  $\text{NH}_3$  oxidation for similar conditions.

Fig. 1 and 2 also show the repeatability of sets 5 and 5R. As can be seen, the reproducibility of the experiments is quite good over the whole temperature range considered, which indicates that the experimental system and the experimental procedure are performing adequately. Fig. S2 to S9 of the Supplementary material (SM) include the reaction path diagrams and sensitivity analysis for  $\text{NH}_3$  and  $\text{H}_2$  consumption for the studied conditions under the highest (40 bar) and lowest (10 bar) studied pressures, when 10 % of the  $\text{NH}_3$  is consumed in any case. Fig. S10 of the supplementary material includes a comparison between the oxidation of  $\text{NH}_3$ ,  $\text{NH}_3/\text{H}_2$  and  $\text{NH}_3/\text{CH}_4$  mixtures.

### 3.2. Effect of stoichiometry ( $\lambda$ ) and composition ( $\text{H}_2/\text{NH}_3$ ratio)

Experimental results show a clear sensitivity to oxygen availability, which has an important effect on  $\text{NH}_3$  consumption and emissions. First, because oxygen is involved in OH radical production and second, because is involved in  $\text{NH}_3$  and  $\text{H}_2$  promoting reactions.  $\text{NH}_3$  and  $\text{H}_2$  conversion starts at a lower temperature at  $\lambda = 3$ , and, where possible,  $\text{NH}_3$  is consumed under oxidizing conditions, Fig. 1 and 2. This is in line with the findings of Dai et al. [16] and Osipova et al. [17], who found that the autoignition of  $\text{NH}_3/\text{H}_2$  mixtures is enhanced by increasing the oxygen excess ratio. The oxygen availability effect is more pronounced in the mixture than for pure  $\text{NH}_3$  [34], under similar experimental conditions.

Increasing the  $\text{H}_2/\text{NH}_3$  ratio also improves the combustion characteristics of  $\text{NH}_3$  due to the increase in H radicals and, consequently the OH radicals through  $\text{H} + \text{O}_2 \rightleftharpoons \text{O} + \text{OH}$  (R12). Under oxidizing conditions and 40 bar, pure  $\text{NH}_3$  starts to convert at 1125 K [34] while when mixed with  $\text{H}_2$ , conversion occurs at 300 K less, (800–825 K for  $\text{H}_2/\text{NH}_3 = 0.5, 1$  and 2). For similar conditions, the  $\text{H}_2/\text{NH}_3$  mixtures also start to convert at lower temperatures than  $\text{CH}_4/\text{NH}_3$  mixtures, where the  $\text{NH}_3$  reaction onset temperature is 875 K, 825 K, and 825 K for 40 bar and  $\text{CH}_4/\text{NH}_3 = 0.5, 1$  and 2 respectively [32]. The oxygen excess ratio and  $\text{H}_2/\text{NH}_3$  ratio also affect  $\text{N}_2\text{O}$  production, which is discussed in the next

section.

### 3.3. $\text{NO}$ , $\text{NO}_2$ and $\text{N}_2\text{O}$ emissions

Fig. 3 shows the  $\text{N}_2\text{O}$  formation peak as a function of temperature. The maximum concentration of  $\text{N}_2\text{O}$  is achieved between 975 and 1025 K in all cases except for the  $\text{H}_2/\text{NH}_3 = 2$  ratio in which it was located between 875 and 1025 K (Fig. S11). However, no significant concentrations of NO or  $\text{NO}_2$  were found at the reactor output (Fig. S12 and S13).

The  $\text{NO}_2$  formed is quickly consumed through  $\text{NO}_2 + \text{H}_2\text{NO} \rightleftharpoons \text{HONO} + \text{HNO}$  (R16) (more accentuated at lower pressures), or  $\text{NO}_2 + \text{H} \rightleftharpoons \text{NO} + \text{OH}$  (R17) particularly as pressure increases, and especially through its reactions with  $\text{NH}_2$  to generate  $\text{H}_2\text{NO} + \text{NO}$  (R18) and  $\text{N}_2\text{O} + \text{H}_2\text{O}$  (R19), the latter responsible for  $\text{N}_2\text{O}$  formation.  $\text{N}_2\text{O}$  consumption occurs mainly through decomposition as the temperature is high enough:  $\text{N}_2\text{O} (+\text{M}) \rightleftharpoons \text{N}_2 + \text{O} (+\text{M})$  (R20) (Fig. S2-S5).

As can be observed in Fig. 3, the formation of  $\text{N}_2\text{O}$  is favored by pressure.  $\text{N}_2\text{O}$  maximum peak is 7 times higher at 40 bar than at 10 bar in the case of 500 ppm  $\text{H}_2$ , contrary to what Wang et al. [25] reported for low pressures (from 1 to 5 bar). For the same  $\text{H}_2$  fraction ( $\text{H}_2/\text{NH}_3 = 1$ ), at  $\lambda = 3$ , the  $\text{N}_2\text{O}$  formation peak is 2 to 4 times higher than for  $\lambda = 1$ , under 40 to 10 bar respectively. Thus, the  $\text{H}_2/\text{NH}_3$  ratio is an influential variable for a given oxygen availability, since an increase in  $\text{H}_2$  leads to an increase of  $\text{N}_2\text{O}$  formation for each pressure studied by a factor of 1.5–2. These results contrast with those found for the oxidation of pure  $\text{NH}_3$ , where no  $\text{N}_2\text{O}$  emissions were found in the same experimental set-up, and similar temperatures and pressures [34].

In the oxidation of  $\text{NH}_3$  mixtures with  $\text{CH}_4$  [32], a  $\text{N}_2\text{O}$  maximum peaks of 140 ppm, 100 ppm, 215 ppm and 290 ppm were respectively reached for the same studied conditions as with  $\text{H}_2$  in the present work, which indicates a consistency of the results. It can be seen that although the  $\text{N}_2\text{O}$  peak formation under the present conditions follows the same trend as in previous work [32], the amount of  $\text{N}_2\text{O}$  formed is lower in the  $\text{H}_2$  mixture compared to the  $\text{CH}_4$  one. Thus, working with higher oxygen excess ratios than 1 is desirable to reduce the unburned  $\text{NH}_3$  despite the higher  $\text{N}_2\text{O}$  production, which is the main drawback of  $\text{NH}_3/\text{H}_2$  oxidation. Thus, from an industrial point of view, the  $\text{NH}_3$  oxidation in its mixtures with  $\text{H}_2$  at high pressure has certain emissions advantages compared to its mixtures with hydrocarbons (e.g.  $\text{CH}_4$ ) as less  $\text{N}_2\text{O}$  production for the same experimental conditions and, as mentioned before, less NO additionally to zero  $\text{CO}_2$  emission. Fig. S11 - S13 of the supplementary material show the  $\text{N}_2\text{O}$ , NO, and  $\text{NO}_2$  conversion for the studied conditions.

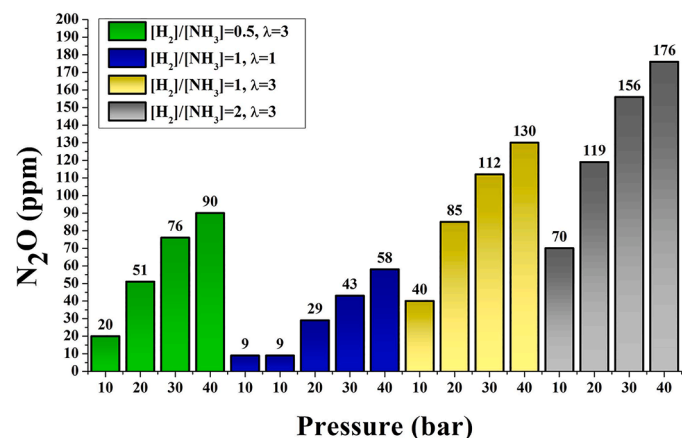


Fig. 3.  $\text{N}_2\text{O}$  production as a function of temperature in all studied conditions, sets 1–16 in Table 1.



### 3.4. Sensitivity analysis

Sensitivity analyses have been performed to identify the most important reactions that control the oxidation of  $\text{NH}_3/\text{H}_2$  mixture, Fig. S6-S9 in supplementary material.  $\text{NH}_3$  and  $\text{H}_2$  consumption are promoted by reactions that produce H through reactions of  $\text{H}_2$  with OH and  $\text{NH}_2$ ,  $\text{NH}_2 + \text{H}_2 \rightleftharpoons \text{NH}_3 + \text{H}$  (-R4) and  $\text{OH} + \text{H}_2 \rightleftharpoons \text{H} + \text{H}_2\text{O}$  (6), and by reaction  $\text{NH}_3 + \text{HO}_2 \rightleftharpoons \text{NH}_2 + \text{H}_2\text{O}_2$  (R21) that produce  $\text{NH}_2$ .  $\text{NH}_3$  and  $\text{H}_2$  consumption are also promoted by reactions that produce OH via  $\text{NH}_2$  reaction with NO (R14) and  $\text{HO}_2$  (R22), through the decomposition of  $\text{H}_2\text{O}_2$  (+M) (R23) which is more relevant under oxidizing conditions and 40 bar, and through the reaction  $\text{H} + \text{O}_2$  (R12) which also produces O radicals and is more important at 10 bar. Finally, some important promoting reactions that lead to the  $\text{HO}_2$  production include:  $\text{H}_2\text{O}_2 + \text{H}$  (R24),  $\text{HNO} + \text{O}_2$  (R25),  $\text{H} + \text{O}_2$  (+M) (R8),  $\text{H}_2\text{NO} + \text{O}_2$  (R26), and to HNO production: the latter one (R26) and  $\text{H}_2\text{NO} + \text{NO}_2$  (R27). It is noted that  $\text{NH}_3$  and  $\text{H}_2$  consumption is promoted by reactions that produce  $\text{NH}_2$ , H, OH, O,  $\text{HO}_2$  and HNO. Under the same experimental conditions, the  $\text{H}_2\text{O}$  production reactions via  $\text{NH}_3 + \text{OH}$  (R3) and via  $\text{NO}_x$  (NO and  $\text{NO}_2$ ) reactions with  $\text{NH}_2$  to form  $\text{N}_2 + \text{H}_2\text{O}$  (R13) and  $\text{N}_2\text{O} + \text{H}_2\text{O}$  (R19), which are favored by pressure, inhibit the consumption of  $\text{NH}_3$  and  $\text{H}_2$ .  $\text{NH}_2$  reactions with  $\text{H}_2\text{NO}$  (R28) and  $\text{HO}_2$  (R29) to form  $\text{NH}_3$ , which are important under oxidizing conditions, also appear as inhibitory reactions. The recombination of  $\text{HO}_2$  (R30) to form  $\text{H}_2\text{O}_2 + \text{O}_2$  which competes with promoting reactions (R21) and (R22) also has a negative impact. We also detected that  $\text{NO}_2$  reactions with H, HNO and  $\text{NH}_2$  to form  $\text{NO} + \text{OH}$  (R17),  $\text{H}_2\text{NO} + \text{NO}$  (R18) and  $\text{NO} + \text{HONO}$  (R31) have an inhibitory behavior, as well as the  $\text{NH}_2$  oxidation to produce  $\text{H}_2\text{NO}$  (R32). It is important to remark that reaction  $\text{H} + \text{O}_2$  (+M) (R8) to form  $\text{HO}_2$ , also appears as inhibitory but only for  $\text{H}_2/\text{NH}_3 = 1$  and 10 bar conditions. It can be concluded that  $\text{NH}_3$  and  $\text{H}_2$  conversion is inhibited by reactions that involve  $\text{H}_2\text{O}$ ,  $\text{NH}_3$ , NO,  $\text{H}_2\text{NO}$  and  $\text{O}_2$  production. According to model calculations, the presence of  $\text{H}_2$  in the  $\text{NH}_3/\text{H}_2$  mixtures makes the influence of O/H radicals to become more significant compared to the conversion of net  $\text{NH}_3$ , even when small amounts of  $\text{H}_2$  are added, as reported in the literature [16,17].

### 3.5. N balance

Fig. 4 shows the N atoms balance of the different experiments to evaluate its quality and to determine if the measured species are dominant under the studied conditions. The N balance is calculated considering the following species:  $\text{NH}_3$ ,  $\text{N}_2$ , NO,  $\text{N}_2\text{O}$ , and  $\text{NO}_2$ . Although NO and  $\text{NO}_2$  have been accounted for in the N balance, these species are around the uncertainty of the equipment below 5 ppm in most cases.

The N balance (in percentage) of the species mentioned calculated with the model is also shown in Fig. 4 as a continuous line that closes at 100% while the experimental N balance closes between 95 and 105% along the whole temperature range. This indicates a great agreement with determined and calculated species and also that the species measured are the predominant ones. Fig. S14 of the SM shows the N balances for the rest of the studied conditions.

## 4. Conclusions

An experimental and simulation study of the oxidation of mixtures of  $\text{NH}_3$  and  $\text{H}_2$  at high pressure (from 10 to 40 bar), under stoichiometric and oxidizing conditions in the 250–1250 K temperature range, in a quartz tubular flow reactor with 1000 ppm of  $\text{NH}_3$  and 500, 1000 and 2000 ppm of  $\text{H}_2$ , using argon as a diluent, has been performed.

The main product of  $\text{NH}_3/\text{H}_2$  mixture conversion is  $\text{N}_2$ , followed by  $\text{N}_2\text{O}$ , while NO and  $\text{NO}_2$  concentrations are negligible and below the detection limit under all the conditions studied. The use of high pressure acts to favor the formation of  $\text{N}_2$  from  $\text{NH}_3$  oxidation compared to what happens at atmospheric pressure. This is a positive outcome for the use of  $\text{NH}_3$  as a fuel in high pressure applications, such as turbines.

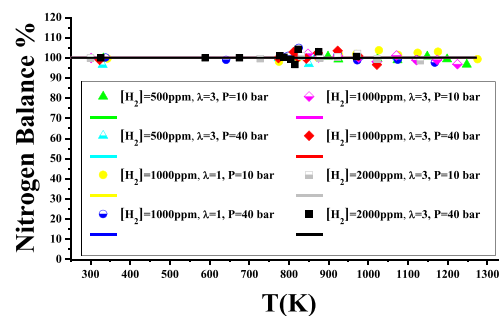


Fig. 4. N balance as a function of temperature, sets 1, 4, 5, 8, 9, 12, 13 and 16 in Table 1.

Nevertheless, the  $\text{N}_2\text{O}$  production in the exhaust gases is significantly higher than in pure  $\text{NH}_3$  oxidation and lower than in  $\text{NH}_3/\text{CH}_4$  mixtures.

The onset of both  $\text{NH}_3$  and  $\text{H}_2$  oxidation occurs at lower temperatures for oxidizing conditions compared to stoichiometric ones, for all the studied pressures, indicating the importance of stoichiometry.

The presence of  $\text{H}_2$  also acts to shift  $\text{NH}_3$  conversion to lower temperatures, up to 250–350 K, compared to pure  $\text{NH}_3$  oxidation.

Pressure has a clear influence on both  $\text{NH}_3$  and  $\text{H}_2$  oxidation regimes, shifting them to a lower temperature as pressure increases. As can be seen, the influence of pressure is more remarkable at low pressures, compared to high ones, and simultaneously this influence is lower at higher  $\text{H}_2/\text{NH}_3$  ratios.

Reactions that produce  $\text{NH}_2$ , H, OH, O,  $\text{HO}_2$  and HNO species favor the  $\text{NH}_3$  and  $\text{H}_2$  consumption. On the other side, inhibition of  $\text{NH}_3$  and  $\text{H}_2$  combustion is powered by reactions that produce  $\text{H}_2\text{O}$ ,  $\text{NH}_3$ , NO,  $\text{H}_2\text{NO}$  and  $\text{O}_2$ , under the studied conditions.

The literature mechanism, used for simulations, is able to describe quite well the  $\text{H}_2$  and  $\text{NH}_3$  conversion trends under most of the studied conditions.

### Novelty and significance statement

The novelty of this research is the experimental and simulated study of ammonia-hydrogen mixtures at high pressure in a plug flow reactor. To our knowledge, there are no previous studies in the literature like the present ones at high pressure (from 10 to 40 bar). It is significant, first of all, because this range of pressures is representative of turbines and engines in the industry and directly helps to understand and improve the implementation of technologies based on carbon-free combustion. Also, the extended database of experimental results of the present work is helpful for model improvement and validation.

### Author contributions

**P.G.:** Designed research, Performed experiments and calculations, Analyzed data, Wrote the manuscript. **M.A.:** Performed experiment. **D.C.:** Performed experiment. **R.B.:** Designed research, Analyzed data, Research Supervision. **M.U.A.:** Designed research, Analyzed data, Research Supervision, Wrote the manuscript.

### Declaration of competing interest

The authors declare that they have no known competing financial interests or personal relationships that could have appeared to influence the work reported in this paper.

### Acknowledgments

The authors acknowledge the funding from the Aragón Government (Ref. T22\_23R), co-funded by FEDER 2014–2020 “Construyendo Europa desde Aragón”, to MINECO and FEDER (Projects RTI2018–098856-B-

I00 and PID2021–124032OB-I00), and MINECO PRE2019–090162 for financial support.

## Supplementary materials

Supplementary material associated with this article can be found, in the online version, at doi:10.1016/j.proci.2024.105726.

## References

- [1] O.I. Awad, B. Zhou, K. Harrath, K. Kadrigama, Characteristics of  $\text{NH}_3/\text{H}_2$  blend as carbon-free fuels: a review, *Int. J. Hydrogen Energy* 48 (2022) 38077–38100.
- [2] H. Kobayashi, A. Hayakawa, K.D.K.A. Somarathne, E.C. Okafor, Science and technology of ammonia combustion, *Proc. Combust. Inst.* 37 (2019) 109–133.
- [3] O. Kurata, N. Iki, T. Matsunuma, T. Inoue, T. Tsujimura, H. Furutani, H. Kobayashi, A. Hayakawa, Performances and emission characteristics of  $\text{NH}_3$ -air and  $\text{NH}_3$ - $\text{CH}_4$ -air combustion gas-turbine power generations, *Proc. Combust. Inst.* 36 (2017) 3351–3359.
- [4] A. Valera-Medina, H. Xiao, M. Owen-Jones, W.I.F. David, P.J. Bowen, Ammonia for power, *Prog. Energy Combust. Sci.* 69 (2018) 63–102.
- [5] A. Yapicioglu, I. Dincer, A review on clean ammonia as a potential fuel for power generators, *Renew. Sustain. Energy Rev.* 103 (2019) 96–108.
- [6] A. Ichikawa, A. Hayakawa, Y. Kitagawa, K.D.K.A. Somarathne, T. Kudo, H. Kobayashi, Laminar burning velocity and Markstein length of ammonia/hydrogen/air premixed flames at elevated pressures, *Int. J. Hydrogen Energy* 40 (2015) 9570–9578.
- [7] E.C. Okafor, K.D.K.A. Somarathne, R. Rathnanan, A. Hayakawa, T. Kudo, O. Kurata, N. Iki, T. Tsujimura, H. Furutani, H. Kobayashi, Control of  $\text{NO}_x$  and other emissions in micro gas turbine combustors fueled with mixtures of methane and ammonia, *Combust. Flame* 211 (2020) 406–416.
- [8] A. Valera-Medina, F. Amer-Hatem, A.K. Azad, I.C. Dedoussi, M. De Joannon, R. X. Fernandes, P. Glarborg, H. Hashemi, X. He, S. Mashruk, J. McGowan, C. Mounaim-Rouselle, A. Ortiz-Prado, A. Ortiz-Valera, I. Rossetti, B. Shu, M. Yehia, H. Xiao, M. Costa, Review on ammonia as a potential fuel: from synthesis to economics, *Energy Fuels* 35 (2021) 6964–7029.
- [9] B. Shu, S.K. Vallabhuni, X. He, G. Issayev, K. Moshhammer, A. Farooq, R. X. Fernandes, A shock tube and modeling study on the autoignition properties of ammonia at intermediate temperatures, *Proc. Combust. Inst.* 37 (2019) 205–211.
- [10] G. Tang, P. Jin, Y. Bao, W.S. Chai, L. Zhou, Experimental investigation of premixed combustion limits of hydrogen and methane additives in ammonia, *Int. J. Hydrogen Energy* 46 (2021) 20765–20776.
- [11] G. Xin, C. Ji, S. Wang, H. Meng, K. Chang, J. Yang, Effect of different volume fractions of ammonia on the combustion and emission characteristics of the hydrogen-fueled engine, *Int. J. Hydrogen Energy* 47 (2022) 16297–16308.
- [12] S.A. Alturaifi, O. Mathieu, E.L. Petersen, A shock-tube study of  $\text{NH}_3$  and  $\text{NH}_3/\text{H}_2$  oxidation using laser absorption of  $\text{NH}_3$  and  $\text{H}_2\text{O}$ , *Proc. Combust. Inst.* 39 (2023) 233–241.
- [13] J.M. Joo, S. Lee, O.C. Kwon, Effects of ammonia substitution on combustion stability limits and  $\text{NO}_x$  emissions of premixed hydrogen-air flames, *Int. J. Hydrogen Energy* 37 (2012) 6933–6941.
- [14] D.H. Um, J.M. Joo, S. Lee, O.C. Kwon, Combustion stability limits and  $\text{NO}_x$  emissions of nonpremixed ammonia-substituted hydrogen-air flames, *Int. J. Hydrogen Energy* 38 (2013) 14854–14865.
- [15] X. Zhang, S.P. Moosakutty, R.P. Rajan, M. Younes, S.M. Sarathy, Combustion chemistry of Ammonia/Hydrogen mixtures: jet-stirred reactor measurements and comprehensive kinetic modeling, *Combust. Flame* 234 (2021) 111653.
- [16] L. Dai, S. Gersen, P. Glarborg, H. Levinsky, A. Mokhov, Experimental and numerical analysis of the autoignition behavior of  $\text{NH}_3$  and  $\text{NH}_3/\text{H}_2$  mixtures at high pressure, *Combust. Flame* 215 (2020) 134–144.
- [17] K.N. Osipova, X. Zhang, S.M. Sarathy, O.P. Korobeinichev, A.G. Shmakov, Ammonia and ammonia/hydrogen blends oxidation in a jet-stirred reactor: experimental and numerical study, *Fuel* 310 (2022) 122202.
- [18] J. Liu, C. Zou, J. Luo, Experimental and modeling study on the ignition delay times of ammonia/methane mixtures at high dilution and high temperatures, *Proc. Combust. Inst.* 39 (2023) 4399–4407.
- [19] M.U. Alzueta, M. Abián, I. Elvira, V.D. Mercader, L. Sieso, Unraveling the NO reduction mechanisms occurring during the combustion of  $\text{NH}_3/\text{CH}_4$  mixtures, *Combust. Flame* 257 (2023) 112531.
- [20] L. Dai, S. Gersen, P. Glarborg, A. Mokhov, H. Levinsky, Autoignition studies of  $\text{NH}_3/\text{CH}_4$  mixtures at high pressure, *Combust. Flame* 218 (2020) 19–26.
- [21] G. Issayev, B.R. Giri, A.M. Elbaz, K.P. Shrestha, F. Mauss, W.L. Roberts, A. Farooq, Combustion behavior of ammonia blended with diethyl ether, *Proc. Combust. Inst.* 38 (2021) 499–506.
- [22] L. Dai, H. Hashemi, P. Glarborg, S. Gersen, P. Marshall, A. Mokhov, H. Levinsky, Ignition delay times of  $\text{NH}_3/\text{DME}$  blends at high pressure and low DME fraction: RCM experiments and simulations, *Combust. Flame* 227 (2021) 120–134.
- [23] G. Yin, J. Li, M. Zhou, J. Li, C. Wang, E. Hu, Z. Huang, Experimental and kinetic study on laminar flame speeds of  $\text{NH}_3/\text{air}$ ,  $\text{NH}_3/\text{H}_2/\text{air}$ ,  $\text{NH}_3/\text{CO}/\text{air}$  under high temperature and elevated pressure, *Combust. Flame* 238 (2022) 111915.
- [24] X. Han, Z. Wang, M. Costa, Z. Sun, Y. He, K. Cen, Experimental and kinetic modeling study of laminar burning velocities of  $\text{NH}_3/\text{air}$ ,  $\text{NH}_3/\text{H}_2/\text{air}$ ,  $\text{NH}_3/\text{CO}/\text{air}$  and  $\text{NH}_3/\text{CH}_4/\text{air}$  premixed flames, *Combust. Flame* 206 (2019) 214–226.
- [25] S. Wang, Z. Wang, W.L. Roberts, Measurements and simulations on effects of elevated pressure and strain rate on  $\text{NO}_x$  emissions in laminar premixed  $\text{NH}_3/\text{CH}_4/\text{air}$  and  $\text{NH}_3/\text{H}_2/\text{air}$  flames, *Fuel* 357 (2024) 130036.
- [26] X. He, B. Shu, D. Nascimento, K. Moshhammer, M. Costa, R.X. Fernandes, Auto-ignition kinetics of ammonia and ammonia/hydrogen mixtures at intermediate temperatures and high pressures, *Combust. Flame* 206 (2019) 189–200.
- [27] M. Pochet, V. Dias, B. Moreau, F. Foucher, H. Jeanmart, F. Contino, Experimental and numerical study, under LTC conditions, of ammonia ignition delay with and without hydrogen addition, *Proc. Combust. Inst.* 37 (2019) 621–629.
- [28] A. Valera-Medina, D.G. Pugh, P. Marsh, G. Bulat, P. Bowen, Preliminary study on lean premixed combustion of ammonia-hydrogen for swirling gas turbine combustors, *Int. J. Hydrogen Energy* 42 (2017) 24495–24503.
- [29] N. Li, H. Deng, Z. Xu, M. Yan, S. Wei, G. Sun, X. Wen, F. Wang, G. Chen, Experimental study on  $\text{NH}_3/\text{H}_2/\text{air}$ ,  $\text{NH}_3/\text{CO}/\text{air}$ ,  $\text{NH}_3/\text{H}_2/\text{CO}/\text{air}$  premix combustion in a closed pipe and dynamic simulation at high temperature and pressure, *Int. J. Hydrogen Energy* 48 (2023) 34551–34564.
- [30] B. Mei, S. Ma, Y. Zhang, X. Zhang, W. Li, Y. Li, Exploration on laminar flame propagation of ammonia and syngas mixtures up to 10 atm, *Combust. Flame* 220 (2020) 368–377.
- [31] Z. Li, S. Li, Kinetic modeling of  $\text{NO}_x$  emissions characteristics of a  $\text{NH}_3/\text{H}_2$  fueled gas turbine combustor, *Int. J. Hydrogen Energy* 46 (2021) 4526–4537.
- [32] P. García-Ruiz, I. Salas, E. Casanova, R. Bilbao, M.U. Alzueta, Experimental and modeling high-pressure study of ammonia-methane oxidation in a flow reactor, submitted for publication 2023.
- [33] J.M. Colom-Díaz, M. Abián, M.Y. Ballester, A. Millera, R. Bilbao, M.U. Alzueta,  $\text{H}_2\text{S}$  conversion in a tubular flow reactor: experiments and kinetic modeling, *Proc. Combust. Inst.* 37 (2019) 727–734.
- [34] P. García-Ruiz, M. Uruén, M. Abián, M.U. Alzueta, High pressure ammonia oxidation in a flow reactor, *Fuel* 348 (2023) 128302.
- [35] L. Marrodán, Á. Millera, R. Bilbao, M.U. Alzueta, An experimental and modeling study of acetylene-dimethyl ether mixtures oxidation at high-pressure, *Fuel* 327 (2022) 125143.
- [36] M.U. Alzueta, V. Mercader, A. Cuoci, S. Gersen, H. Hashemi, P. Glarborg, Flow reactor oxidation of ammonia-hydrogen fuel mixtures, *Energy Fuels* 38 (2024) 3369–3381.
- [37] Ansys Chemkin-Pro, Chemical Kinetics Simulation Software, |, Chemkin ANSYS, Chemkin, 2023. R1, Nov. 2022.